

## Supporting information

### A bimodal anionic MOF: Turn-off sensing for Cu<sup>II</sup> and specific sensitization of Eu<sup>III</sup>

Sohini Bhattacharyya <sup>a</sup>, Anindita Chakraborty <sup>a</sup>, Kolleboyina Jayaramulu <sup>a</sup>, Arpan Hazra <sup>a</sup>,  
and Tapas Kumar Maji <sup>a</sup> \*

<sup>a</sup> Molecular Materials Laboratory, Chemistry and Physics of Materials Unit, Jawaharlal Nehru  
Centre for Advanced Scientific Research, Jakkur, Bangalore 560 064, India

#### Materials

All the reagents and solvent were used as obtained from commercial supplies without any further purification. 1,4-Naphthalene dicarboxylic acid(ndc) and the metal salts used were procured from Alfa Aesar and Aldrich Co. Ltd. respectively.

#### Synthesis of [Mg<sub>3</sub>(ndc)<sub>2.5</sub>(HCO<sub>2</sub>)<sub>2</sub>(H<sub>2</sub>O)(NH<sub>2</sub>Me<sub>2</sub>)]2H<sub>2</sub>O.DMF (**1**) :

Mg(NO<sub>3</sub>)<sub>2</sub>.6H<sub>2</sub>O(1mmol, 256mg) and 1,4-ndc(1mmol, 216mg) were mixed well in 20 ml DMF. Then a few drops of water were added and the mixture was sonicated for 10mins. The resulting mixture was transferred into a Teflon sealed autoclave and the system was kept at 120°C for two days. On cooling colourless single crystals of **1** were obtained. Yield:76%; relative to Mg(II). Anal. Calculated for C<sub>37</sub>H<sub>37</sub>Mg<sub>3</sub>O<sub>18</sub>N<sub>2</sub>: H:4.28 C:51.04 N: 3.22% Found: H: 4.12 C: 51.63 N:3.27%

The phase purity was checked by comparing the PXRD pattern (Figure S3) of the bulk powder sample with the simulated data from single-crystal data.

#### Physical Measurements

The elemental analysis was carried out using a Thermo Fischer Flash 2000 Elemental Analyzer. Thermogravimetric analysis (TGA) was carried out (Mettler Toledo) in nitrogen atmosphere (flow rate = 50 ml min<sup>-1</sup>) in the temperature range 30 – 550 °C (heating rate = 3°C min<sup>-1</sup>). Powder XRD pattern was recorded by using Cu-K $\alpha$  radiation (Bruker D8 Discover; 40 kV, 30 MA). Electronic absorption spectra were recorded on a Perkin Elmer Lambda 750 UV-VIS-NIR Spectrometer and emission spectra were recorded on Perkin

Elmer Ls 55 Luminescence Spectrometer. Solid state UV spectrum was recorded in reflectance mode. IR spectra of the compounds were recorded on a Bruker IFS 66v/S spectrophotometer using the KBr pellets in the region 4000–400  $\text{cm}^{-1}$ . Inductively Coupled Plasma-Optical Emission Spectroscopy (ICP-OES) measurements were recorded on Perkin Elmer Optima 7000dv ICP-OES.

### Crystallography:

A suitable single crystal of compound **1** was mounted on a thin glass fiber with commercially available super glue. X-ray single crystal structural data were collected on a Bruker Smart-CCD diffractometer equipped with a normal focus, 2.4 kW sealed tube X-ray source with graphite monochromated Mo-K $\alpha$  radiation ( $\lambda = 0.71073 \text{ \AA}$ ) operating at 50 kV and 30 mA.

The program SAINT<sup>1</sup> was used for the integration of diffraction profiles and absorption correction was made with SADABS<sup>2</sup> program. All the structures were solved by SIR 92<sup>3</sup> and refined by full matrix least square method using SHELXL.<sup>4</sup> All the hydrogen atoms were fixed by HFIX and placed in ideal positions. There is a disordered ndc molecule where the naphthalene ring has a positional disorder over two positions. Detailed structural investigation shows the presence of an inversion center (as observed using Mercury 3.3) resulting in the disordered ndc molecule and due to this positional disorder carbon atoms with half occupancy were observed on both sides of the central benzene ring.

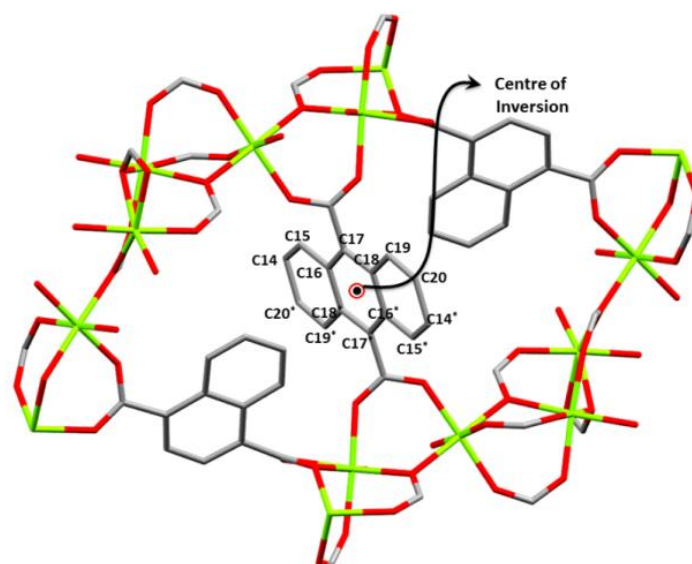


**Fig. S1:** One disordered ndc linker in the framework of **1** is shown with an inversion center.

The occupancy of carbon atoms was set to free and the value was found to be ~0.5 after SHELXL refinement. Then the occupancy of the carbon atoms constructing the naphthalene ring was assigned to the value of 0.5 which gives a stable result after the SHELXL

refinement. For better understanding, we have drawn the figure where it is clear that the formation of 9,10-anthracene-dicarboxylate like moiety is due to the overlap of two ndc molecules. Throughout the structure, two NDC molecules (red and blue according to the structure) have positioned themselves in two different orientations (50:50 ratio) which is reflected from the presence of electron density both the side of benzene ring (containing the dicarboxylate) of the ndc molecule.

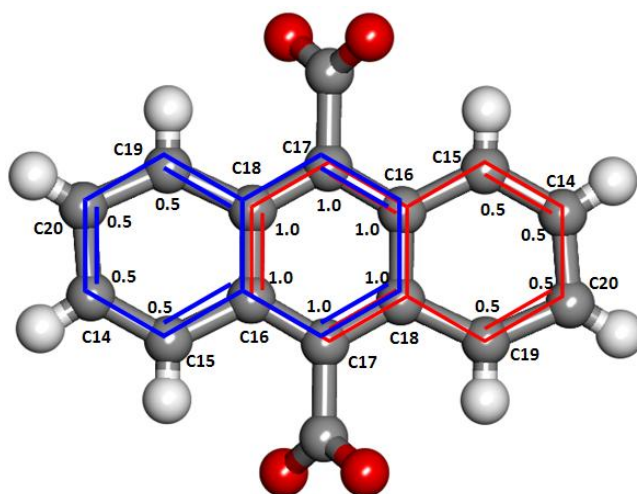


**Fig. S2:** Positional disorder in ndc is shown in two different colours, red and blue.

There is also a disordered water molecule located in two different positions (in a distance of 1.79Å) with equal probability. This has been demarcated as O2w and O2wa. PART command was used to obtain a perfect model to describe this disordered guest water molecule.

Potential solvent accessible area or void space was calculated using the PLATON<sup>5</sup> multipurpose crystallographic software. All crystallographic and structure refinement data of **1** is summarized in Table 1. All calculations were carried out using SHELXL 97,<sup>4</sup> PLATON,<sup>5</sup> SHELXS 97<sup>4</sup> and WinGX system, Ver 1.80.05.<sup>6</sup>

**Table S1.** Crystal Data and Structure Refinement for [Mg<sub>3</sub>(ndc)<sub>2.5</sub>(HCO<sub>2</sub>)<sub>2</sub>(H<sub>2</sub>O)(NH<sub>2</sub>Me<sub>2</sub>)  
]2H<sub>2</sub>O.DMF (CCDC number: 1017348)

<b>Parameter</b>	<b>1</b>
Empirical formula	C <sub>37</sub> H <sub>37</sub> Mg <sub>3</sub> O <sub>18</sub> N <sub>2</sub>
Formula weight	870.61
Crystal system	<i>Monoclinic</i>
Space group	<i>P21/c</i> (No.14)
<i>a</i> , Å	11.3593(4)
<i>b</i> , Å	22.5823(8)
<i>c</i> , Å	16.5923(5)
$\beta$ , deg	92.129(2)
<i>V</i> , Å <sup>3</sup>	4253.3(2)
<i>Z</i>	4
<i>T</i> , K	120
$\mu$ , mm <sup>-1</sup>	0.147
<i>D</i> <sub>calcd</sub> , g/cm <sup>3</sup>	1.353
<i>F</i> (000)	1796
reflections [ <i>I</i> >2 $\sigma$ ( <i>I</i> )]	3619
unique reflections	7457
measured reflections	57145
<i>R</i> <sub>int</sub>	0.185
GOF on <i>F</i> <sup>2</sup>	1.01
<i>R</i> <sub>1</sub> [ <i>I</i> >2 $\sigma$ ( <i>I</i> )] <sup>[a]</sup>	0.0992
<i>R</i> <sub>w</sub> [ <i>I</i> >2 $\sigma$ ( <i>I</i> )] <sup>[b]</sup>	0.2988

$$(R = \sum||F_o|-|F_c||/\sum|F_o|, R_w = [\sum\{w(F_o^2 - F_c^2)^2\}/\sum\{w(F_o^2)^2\}]^{1/2})$$

**Table S2.** Selected bond distances (Å) for **1**.

Mg1-O1	2.011(5)	Mg2-O13	2.047(5)
Mg1-O6	2.036(5)	Mg2-O9	2.023(5)
Mg1-O11	2.114(5)	Mg2-O3	2.125(5)
Mg1-O13	2.134(5)	Mg2-O4	2.183(5)
Mg1-O7	2.063(5)	Mg2-O12	2.041(5)
Mg1-O10	2.083(5)	Mg3-O2	2.040(5)
Mg2-O5	2.046(5)	Mg3-O8	2.060(5)

**Table S3.** Selected bond angles (°) of Compound **1**.

O1-Mg1-O6	176.4(2)	O3-Mg2-O12	90.7(2)
O1-Mg1-O7	90.7(2)	O4-Mg2-O12	91.9(2)
O1w-Mg3-O2	88.8(2)	O3-Mg2-O5	88.1(2)
O1-Mg1-O11	91.3(2)	O6-Mg1-O11	91.3(2)
O2-Mg3-O8	90.9(2)	O4-Mg2-O5	85.0(2)
O1w-Mg3-O11	177.0(2)	O1-Mg1-O10	91.3(2)

**TGA of 1 and Cu<sup>II</sup>@1' (Fig S5):**

The initial ~6% weight loss correspond to one coordinated water and 2 guest water molecules till 100°C. Next ~ 8% weight loss till 170°C corresponds to one DMF molecule. Beyond this the framework starts decomposing continuously. For **Cu<sup>II</sup>@1'**, the framework is stable till 250°C after an initial loss of 2%.

**Preparation of Sample for Adsorption:**

Adsorption isotherms of CO<sub>2</sub> at 195 K and N<sub>2</sub> at 77 K were recorded with the dehydrated sample using QUANTACHROME QUADRASORB-SI analyzer. To prepare the dehydrated sample of **1** (**1'**) approximately 100 mg of sample was taken in a sample holder and degassed at 110°C under 10<sup>-1</sup> pa vacuum for about 12hours prior to the measurements. Dead volume of the sample cell was measured using helium gas of 99.999% purity. The amount of gas adsorbed was calculated from the pressure difference ( $P_{cal} - P_e$ ), where  $P_{cal}$  is the calculated

pressure with no gas adsorption and  $P_e$  is the observed equilibrium pressure. All the operations were computer-controlled and automatic.

- For preparing the different metal ion exchanged compounds, **1** is activated at 110°C under high vacuum overnight before immersing it in the respective metal ion solutions.

#### **Preparation of $M^{II}@1'$ and $Ln^{III}@1'$ :**

50mg of activated **1**(**1'**) is immersed in 30ml 0.01M  $M^{II}$  (where M is any transition metal) solutions in ethanol for 7 days and the solution is changed daily within these 7 days. For Stern-Volmer plots, **1'** is dipped in standard solutions for 7 days as mentioned in the main text. Then it is washed repeatedly with ethanol. For  $Ln^{III}@1'$ , 0.01M solutions of nitrates of  $Eu^{III}$ ,  $Dy^{III}$ ,  $Tb^{III}$  and  $Sm^{III}$  are used in the same way.

#### **Stern-Volmer Plots**

According to the Stern-Volmer equation,

$$\frac{I_0}{I} = 1 + K_{sv}[Q]$$

where  $I_0$ =initial fluorescence intensity without any quencher

$I$ = emission intensity in the presence of quencher

$[Q]$ = quencher concentration

$K_{sv}$  = Stern-Volmer quenching constant

Emission intensity of **1** exchanged with different concentrations of  $Cu^{II}$  solution is measured and the Stern-Volmer Plot is constructed to obtain the quenching constant. The same experiment has been repeated at 80°C.

**Table S4:** ICP-MS data for cation exchange in a mixture (0.01M of each metal cation).

Sl. No.	Cation	Number of Cations per Formula Unit	Maximum Number of Cations Possible per Formula Unit	% Exchange of Cation with DMA
1	$Mn^{II}$	0	0.5	0.0

2	Co <sup>II</sup>	0.016	0.5	3.2
3	Ni <sup>II</sup>	0.090	0.5	17.9
4	Cu <sup>II</sup>	0.423	0.5	84.5
5	Zn <sup>II</sup>	0	0.5	0.0

### **Calculation of Cu<sup>II</sup> Inclusion from UV Spectra of Supernatant:**

First the UV spectrum of a  $6.25 \times 10^{-4}$  M Cu<sup>II</sup> solution in ethanol is recorded. **1'** is dipped in it for 7 days and the UV spectrum of the resultant supernatant solution is recorded. Using Lambert-Beer's Law, from the decrease in the absorbance, we calculated the decrease in the concentration of the Cu<sup>II</sup> solution and found ~84.5% exchange with Cu<sup>II</sup> cation, which is in accordance with the ICP data (Fig S7).

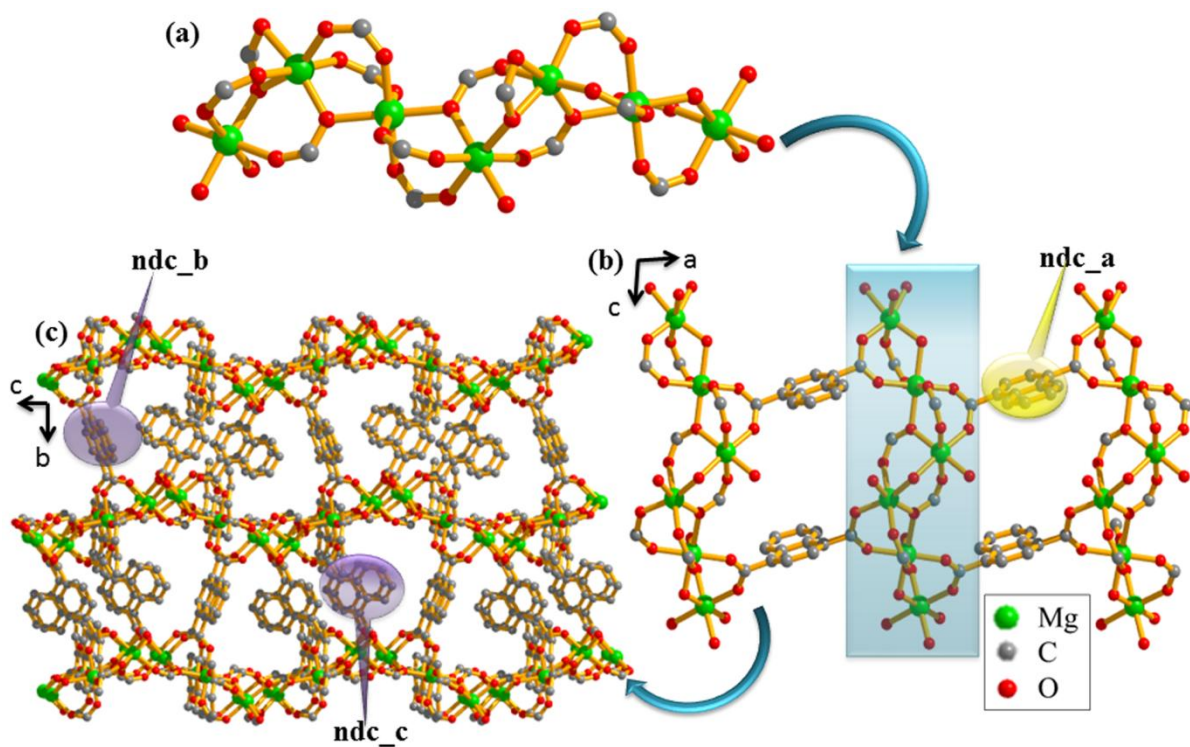


**Fig. S3** (a) 1D chain of **1** along crystallographic *c* direction. (b) 2D sheet of **1** along the crystallographic *ac* plane. (c) View of 3D network of **1** along crystallographic *a* axis.

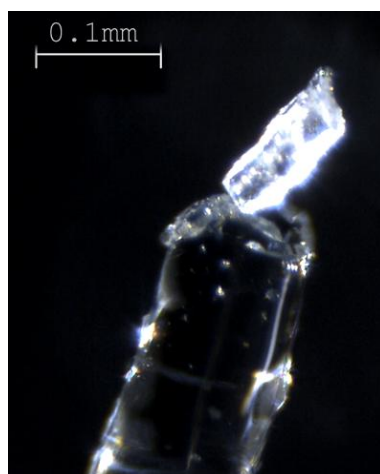


**Fig. S4** Single crystal of **1** on a glass fiber and the scale bar indicating the size of the crystal.

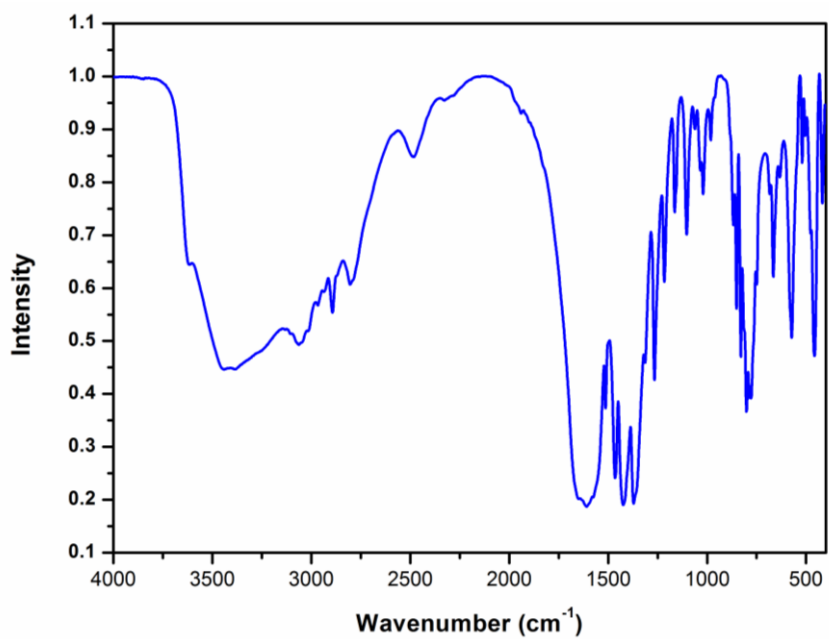


**Fig. S5** IR spectrum of **1**.

**Table S5:** Principal Peaks in IR (Fig S2).

Peak Position	Nature	Vibration
1640cm <sup>-1</sup>	strong	C=O stretch
795cm <sup>-1</sup>	strong	Aromatic C-H stretch
1269, 1374cm <sup>-1</sup>	strong	C-N stretch
2809, 3063cm <sup>-1</sup>	strong, broad	N-H stretch

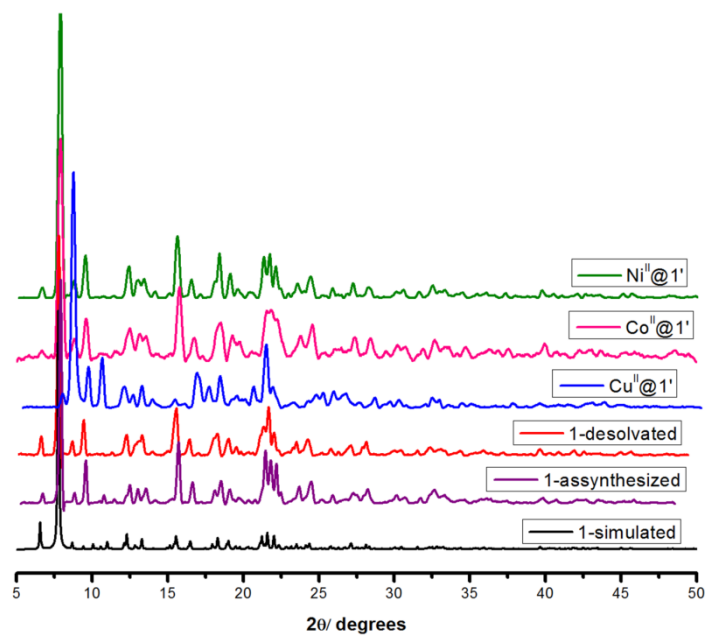


**Fig. S6** PXRD patterns of **1** and **M<sup>II</sup>@1'**, (where M<sup>II</sup> is a transition metal cation).

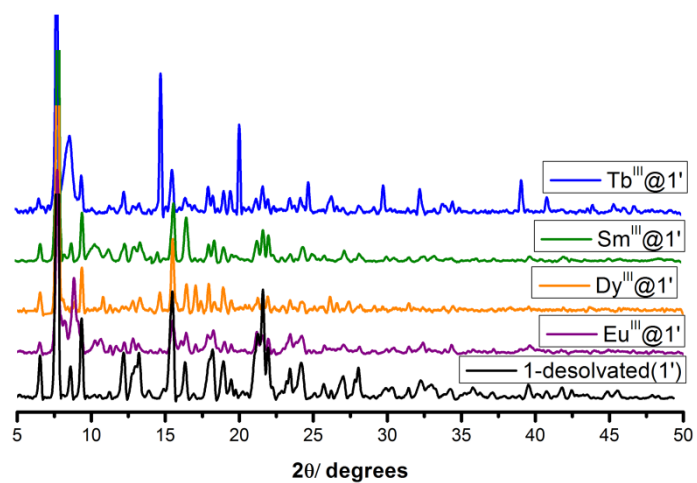


**Fig. S7** PXRD patterns of **1** and **Ln<sup>III</sup>@1'**, (where Ln<sup>III</sup> is a lanthanide cation)

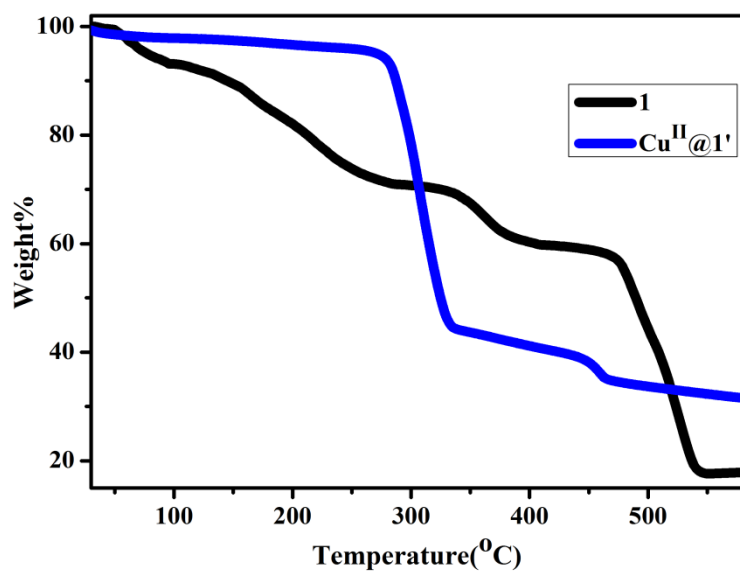


Fig. S8 TGA profile for **1** and **Cu<sup>II</sup>@1'**.

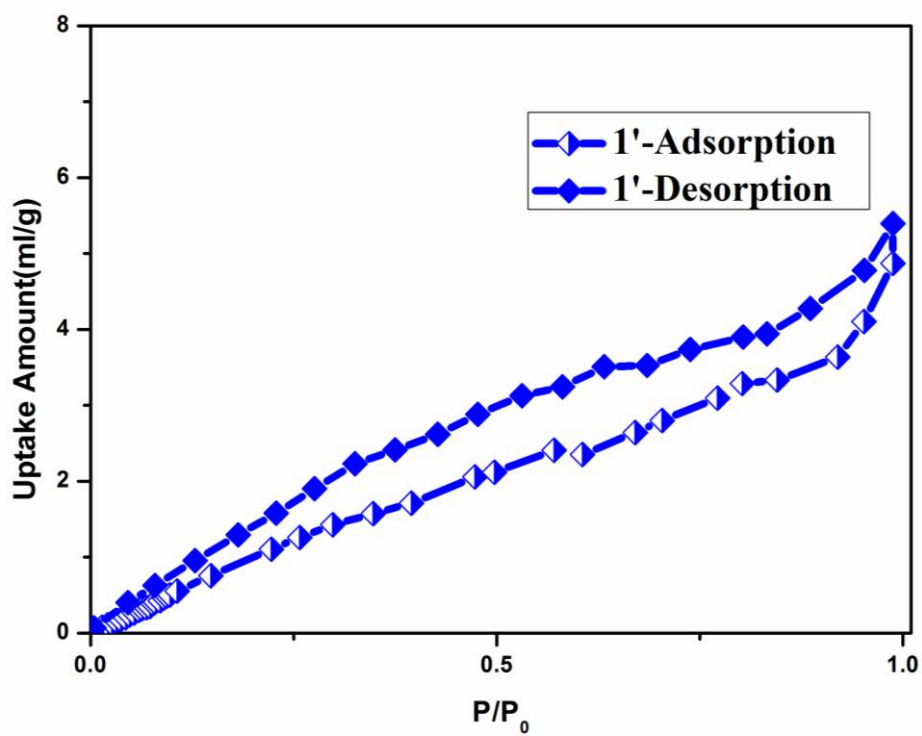
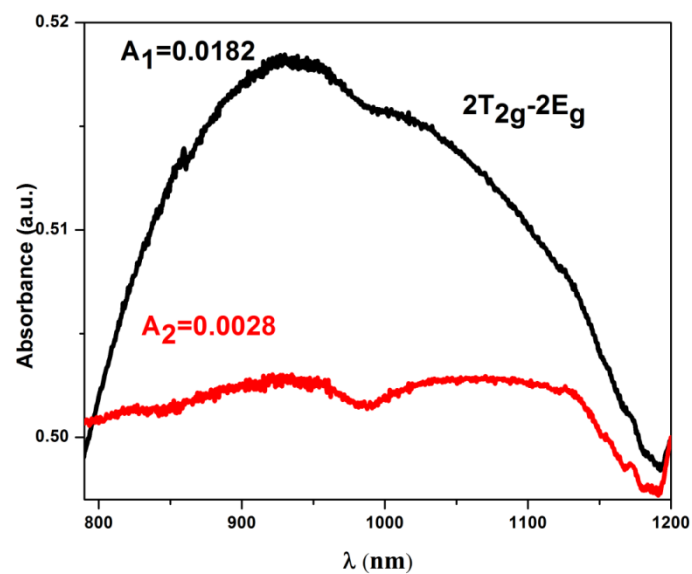
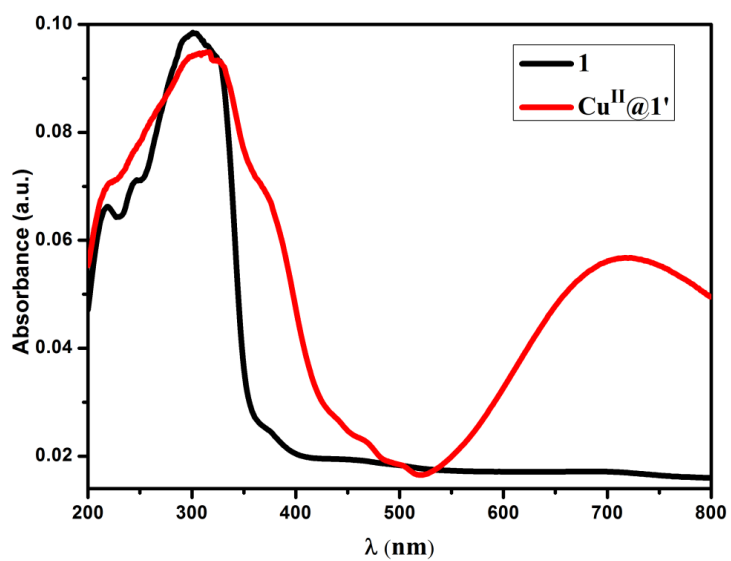


Fig. S9 N<sub>2</sub> Adsorption-desorption isotherm for **1'** at 77 K.



**Fig. S10** UV-VIS spectra: (Black)  $\text{Cu}^{\text{II}}$  solution of  $6.25 \times 10^{-4}$  (M) and (Red)  $\text{Cu}^{\text{II}}$  solution obtained after immersing **1'** for 7 days.



**Fig. S11** UV-vis spectra of solid **1** and  $\text{Cu}^{\text{II}}@1'$ .

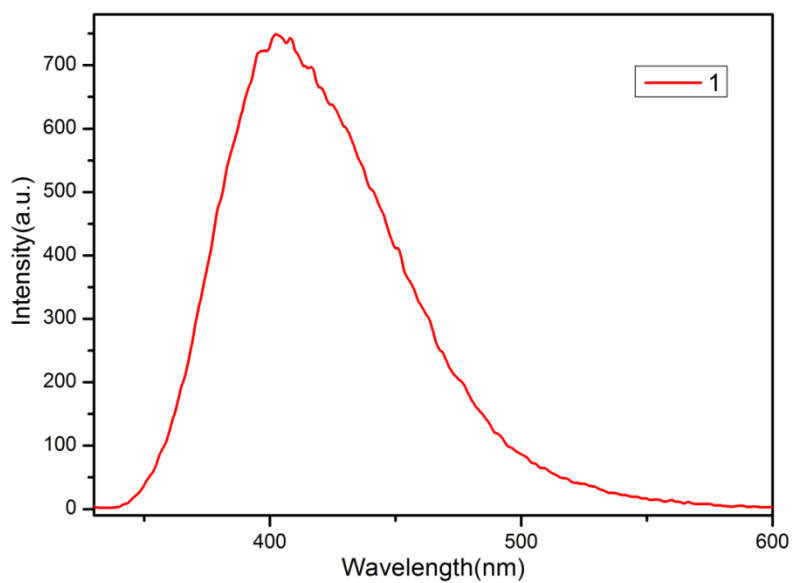


**Fig. S12** Emission spectrum of **1**, excited at 317nm.

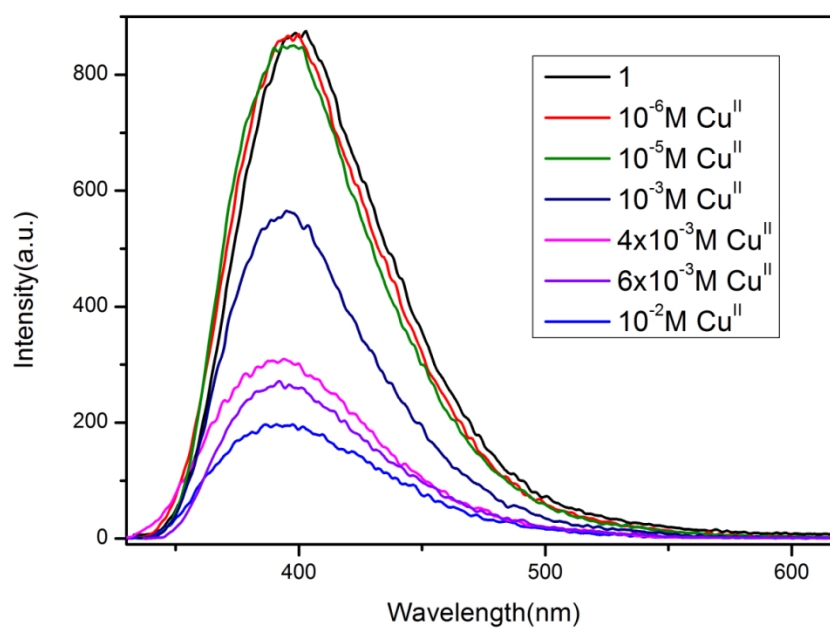


**Fig. S13** Emission spectra of **Cu<sup>II</sup>@1** obtained from different concentrations of **Cu<sup>II</sup>** at 80°C showing quenching of fluorescence of **1**.

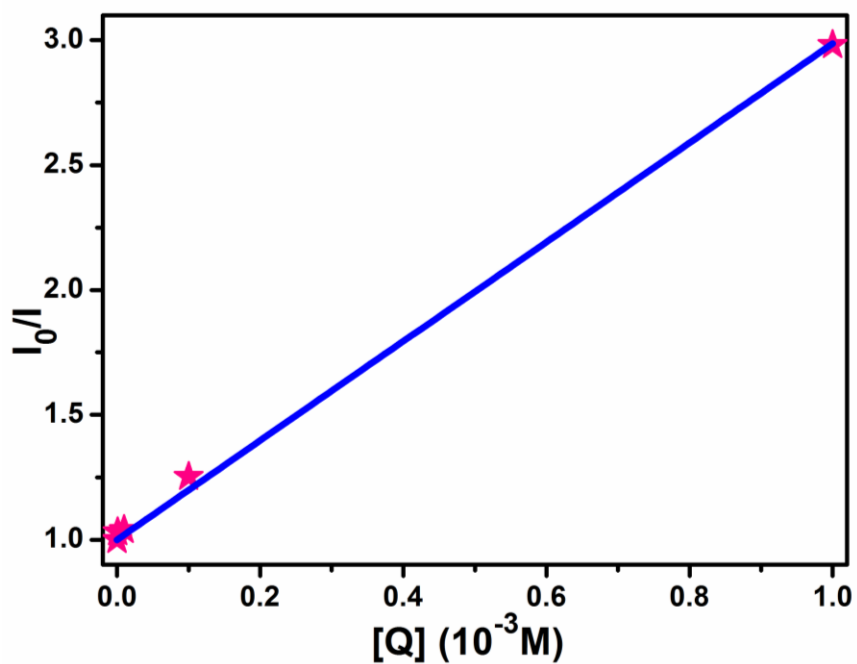


**Fig. S14** Stern-Volmer plot constructed for quenching of the emission of **1** by  $\text{Cu}^{\text{II}}$  at 80 °C. Here the plot has been constructed for  $[Q]=0, 10^{-9}, 10^{-6}, 10^{-5}, 10^{-4}, 10^{-3}(M)$ .

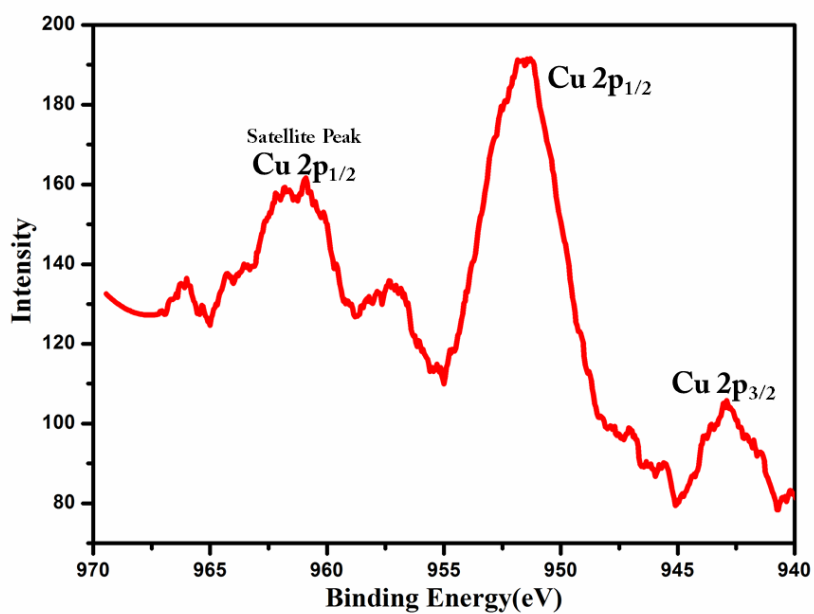


**Fig. S15** XPS data for Cu 2p in  $\text{Cu}^{\text{II}}@1$ .

The XPS analysis clearly shows the different peaks for Cu 2p<sub>3/2</sub> and 2p<sub>1/2</sub>, implying ligand field splitting of the d-orbitals of Cu in **Cu<sup>II</sup>@1'**. The peak at 943.5eV implies that Cu<sup>II</sup> is present.

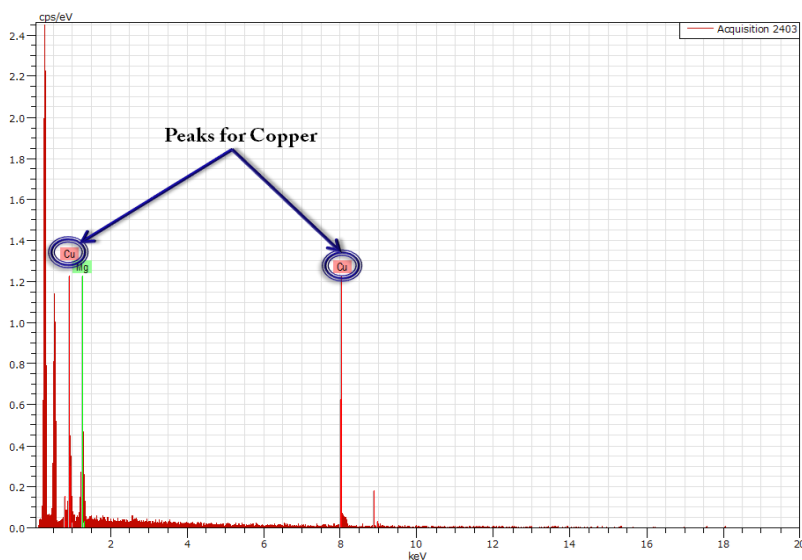


**Fig. S16** EDS analysis of **Cu<sup>II</sup>@1'**. Peaks for Cu in the EDS analysis plot has been marked.

#### References:

1. S. V. a. SMART (V 5.628), XPREP, SHELXTL; Bruker AXS Inc. Madison, Wisconsin, USA, 2004.
2. G. M. Sheldrick, *SADABS, Empirical Absorption Correction Program, University of Göttingen, Göttingen, 1997.*
3. A. Altomare, G. Casciarano, C. Giacovazzo and A. Guagliardi, *J. Appl. Crystallogr.*, 1993, **26**, 343-350.
4. G. M. Sheldrick, *SHELXL 97, Program for the Solution of Crystal Structure, University of Göttingen, Germany, 1997.*
5. A. Spek, *J. Appl. Crystallogr.*, 2003, **36**, 7-13.
6. L. Farrugia, *J. Appl. Crystallogr.*, 1999, **32**, 837-838.